Impact of plasma jet vacuum ultraviolet radiation on reactive oxygen species generation in bio-relevant liquids

H. Jablonowski, R. Bussiahn, M. U. Hammer, et al.

View Online · **Export Citation** · **CrossMark**

ARTICLES YOU MAY BE INTERESTED IN

Perspective: The physics, diagnostics, and applications of atmospheric pressure low temperature plasma sources used in plasma medicine
Journal of Applied Physics **122**, 020901 (2017); https://doi.org/10.1063/1.4993710

Identification of the biologically active liquid chemistry induced by a nonthermal atmospheric pressure plasma jet
Biointerphases **10**, 029518 (2015); https://doi.org/10.1116/1.4919710

Atmospheric pressure plasma jet in Ar and Ar/H_2O mixtures: Optical emission spectroscopy and temperature measurements
Physics of Plasmas **17**, 063504 (2010); https://doi.org/10.1063/1.3439685

Impact of plasma jet vacuum ultraviolet radiation on reactive oxygen species generation in bio-relevant liquids

H. Jablonowski,[1,2] R. Bussiahn,[2] M. U. Hammer,[1,2] K.-D. Weltmann,[2] Th. von Woedtke,[2] and S. Reuter[1,2]

[1]*Center for Innovation Competence plasmatis, Felix-Hausdorff-Str. 2, 17489 Greifswald, Germany*
[2]*Leibniz Institute for Plasma Science and Technology, INP Greifswald e.V. Felix-Hausdorff-Str. 2, 17489 Greifswald, Germany*

Plasma medicine utilizes the combined interaction of plasma produced reactive components. These are reactive atoms, molecules, ions, metastable species, and radiation. Here, ultraviolet (UV, 100–400 nm) and, in particular, vacuum ultraviolet (VUV, 10–200 nm) radiation generated by an atmospheric pressure argon plasma jet were investigated regarding plasma emission, absorption in a humidified atmosphere and in solutions relevant for plasma medicine. The energy absorption was obtained for simple solutions like distilled water (dH_2O) or ultrapure water and sodium chloride (NaCl) solution as well as for more complex ones, for example, Rosewell Park Memorial Institute (RPMI 1640) cell culture media. As moderate stable reactive oxygen species, hydrogen peroxide (H_2O_2) was studied. Highly reactive oxygen radicals, namely, superoxide anion ($O_2^{\bullet-}$) and hydroxyl radicals ($^\bullet OH$), were investigated by the use of electron paramagnetic resonance spectroscopy. All species amounts were detected for three different treatment cases: Plasma jet generated VUV and UV radiation, plasma jet generated UV radiation without VUV part, and complete plasma jet including all reactive components additionally to VUV and UV radiation. It was found that a considerable amount of radicals are generated by the plasma generated photoemission. From the experiments, estimation on the low hazard potential of plasma generated VUV radiation is discussed. © *2015 Author(s). All article content, except where otherwise noted, is licensed under a Creative Commons Attribution 3.0 Unported License.*
[http://dx.doi.org/10.1063/1.4934989]

I. INTRODUCTION

In the past decades, atmospheric pressure plasma jets have been increasingly used for the new field of plasma medicine.[1–5] The strongly non-equilibrium chemistry along with their physical properties of energy transfer into sensible surfaces makes them excellently suited for treatment of, e.g., chronic wounds.[6–9] The energy dissipated within the plasma is transferred into thermal, chemical, electronic, and radiative energy, to name the most relevant examples. The gas and plasma phase chemistry of these jets has been investigated quite thoroughly, and many processes have been already understood.[10–13] For the field of plasma medicine, however, a further diagnostic step is required: When biological systems are plasma treated, these systems usually require a liquid surrounding, such as cell culture medium for in vitro studies.[14] Also under physiological conditions *in vivo*, a liquid environment nearly always surrounds living tissue. It is in this liquid surrounding that the reactive species generation processes have to be diagnosed and understood. The present study focuses on the generation of reactive species by vacuum ultraviolet (VUV) light, emitted from the plasma jet.[15,16]

Fig. 1 shows a simple but very evident experiment: the argon atmospheric plasma jet kinpen09, used in this study, is directed onto a magnesium fluoride (MgF_2) window, which transmits light down to a wavelength of 115 nm. On the backside of the window, a VUV active phosphor is applied. In the right side of the picture, a quartz disc is positioned on top of the MgF_2 window, which only transmits light of a wavelength greater than 250 nm. The shadowing of the phosphorescence exposes two effects: (a) the radiation responsible for the phosphorescence is VUV, and not ultraviolet UV radiation; (b) the radiation originates from the plasma jet.

VUV radiation is absorbed in ambient air. However, it can reach a target, if emitted from a noble gas plasma jet. The feed gas atmosphere will guide the radiation to greater distances as has been shown for a large jet for distances up to 10 cm (see Ref. 11). Even at larger distances, this radiation
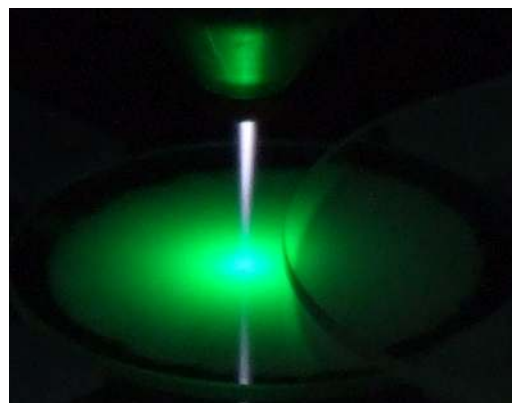

FIG. 1. Plasma jet kinpen09 (with visible plasma plume), VUV emission profile of the kinpen09 in a phosphorescing film and blocking of VUV light by a quartz disc (right).

TABLE I. Bond dissociation energies for biologically relevant molecules and their corresponding wavelength.

	Bond dissociation energy		Wavelength
	kJ/mol	eV	nm
$HO_2 \rightarrow H + O_2$	197.0[18]	2.04	607.8
$NH \rightarrow N + H$	356.0[18]	3.69	336.0
$H_2O_2 \rightarrow HO_2 + H$	374.5[18]	3.88	319.5
$OH \rightarrow O + H$	428.0[18]	4.44	279.2
$H_2 \rightarrow 2H$	435.9[18]	4.52	274.3
$O_2 \rightarrow 2O$	498.3[18]	5.16	240.3
$H_2O \rightarrow OH + H$	498.7[18]	5.17	239.8
$CO_2 \rightarrow CO + O$	532.2[18]	5.52	224.6
$NO \rightarrow N + O$	631.6[19]	6.55	189.3
$N_2 \rightarrow 2N$	945.4[18]	9.80	126.5
$CO \rightarrow C + O$	1076.5[18]	11.16	111.1

can still be the cause for significant photochemistry in the gas and liquid phase. Therefore, it can be assumed that VUV radiation could also reach the cells. It was shown in Ref. 11 that a considerable amount of atomic oxygen could originate from photo-dissociation by VUV radiation. Especially for small molecules relevant in cell signaling and for the interaction with biomolecules, the dissociative energy threshold is within the photon energy of ultraviolet and vacuum ultraviolet ((V)UV) radiation emitted by plasma jets[17] (see Table I).

From Table I, it becomes clear that plasma jet's VUV photons carry enough energy onto treated liquids, to contribute to the reactive chemistry initiated within the liquids.

In the present study, the aim is to identify the VUV radiation as well as its possible impact on liquids surrounding cells. Furthermore, the amount of VUV radiation emitted from the plasma jet is quantified. The absorption of VUV radiation—in this case generated by a deuterium lamp—by different biologically relevant liquids is studied. Finally, the reactive oxygen species (ROS) generating effect of plasma generated VUV radiation absorption within the liquids is investigated on the example of hydroxyl ($^\bullet OH$), and superoxide anion ($O_2^{\bullet -}$) radicals, as well as hydrogen peroxide (H_2O_2). Also for these investigations, various liquids were used. The aim was not only to study the production of reactive species by VUV radiation within plasma treated liquids but also to investigate the effect of diverse biologically relevant liquids on the absorption spectrum.

II. MATERIALS AND METHODS

A. Investigated liquids

In this study, the used liquids were distilled or ultrapure water, respectively, physiological sodium chloride solution (0.9% NaCl, Sigma-Aldrich, USA), Hank's balanced salt solution (HBSS, Lonza, Switzerland), Sørensen's phosphate buffer (SPB, Lonza, Switzerland), Dulbecco's phosphate buffer (DPBS, Lonza, Switzerland), Iscove's modified Dulbecco's medium (IMDM, Lonza, Switzerland), EpiLife (LifeTechnology, Germany), and Roswell Park Memorial Institute (RPMI 1640) cell culture medium from Lonza (Switzerland). Physiological sodium chloride solution is commonly used in medicine as intravenous infusion as well as to flush wounds and skin abrasions. HBSS is a commonly used buffer system in cell culture systems, which are exposed to atmospheric conditions instead of carbon dioxide (CO_2) incubation. Sørensen's phosphate buffer is used in clinics and laboratories if a phosphate buffer with a pH between 5.8 and 8 is needed.

IMDM and RPMI are commonly used cell culture media; they contain two buffer systems, one phosphate buffer system and one bicarbonate system (see Table II), but RPMI differs from other mammalian cell culture media in its pH 8. EpiLife is a cell culture medium for long-term, serum-free culture of human epidermal keratinocytes and human corneal epithelial cells.

B. Plasma source

For the study, an rf atmospheric pressure argon plasma jet, the so called kinpen09 (neoplas GmbH Greifswald, Germany) was used. This plasma jet is a pin type dielectric barrier plasma jet with an outer, grounded ring electrode.[20] The diameter of the nozzle exit is 1.6 mm. The plasma jet is operated with 3 standard liters per minute (slm) argon (purity 99.999%). The operating frequency is in the order of 1 MHz and its amplitude is in the range of 2–6 kV_{pp}.[20] For the treatment, a nozzle to window distance of 9 mm was used. The plasma jets dynamic is characterized by moving ionization waves[12] which are guided by the argon air boundary.[21] The discharge pathway is therefore mainly through argon, and one dominant emission characteristics thus originates from the argon excimer emission, studied in the present work.

TABLE II. Composition of the investigated liquids, sorted by complexity, starting with distilled water or ultrapure water to full cell culture media.

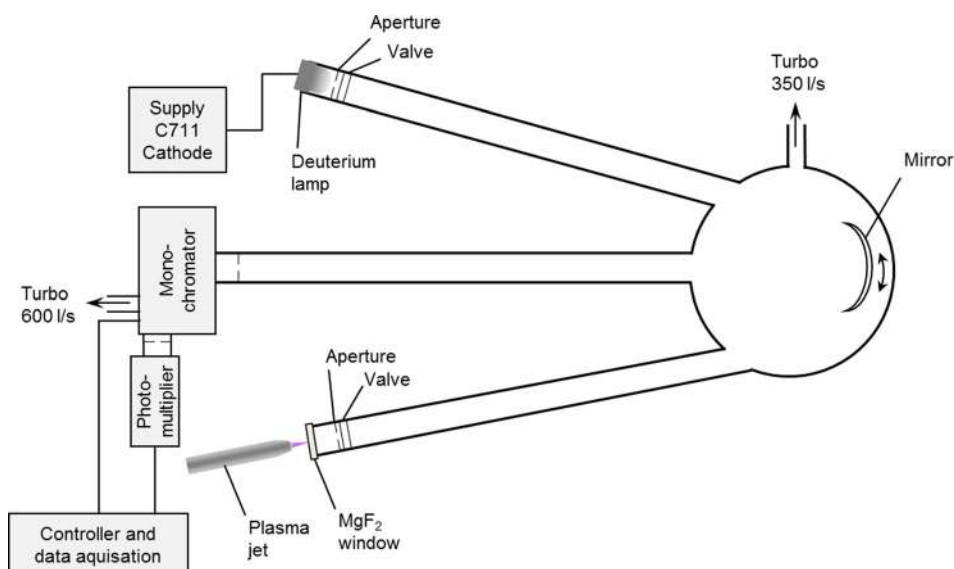|	Inorganic salts	buffer	Glucose	Amino acids	Vitamins	HEPES	Fe, Cu,…	Glutathione
dH$_2$O	−	−	−	−	−	−	−	−
SPB	+	+	−	−	−	−	−	−
DPBS	+	+	−	−	−	−	−	−
Hank's BSS	+	+	+	−	−	−	−	−
IMDM	+	+	+	+	+	+	−	−
Epilife	+	+	+	+	+	+	+	−
RPMI	+	+	+	+	+	−	+	+

FIG. 2. VUV spectroscopy setup with plasma jet.

C. Optical emission spectroscopy

For the VUV emission and absorption measurements, a setup described in Refs. 15 and 16 was used (see Fig. 2). It consists of a VUV-monochromator with 0.5 m focal length and a 1200 g/mm grating. The spectrograph is optically connected to the plasma jet via a spherical mirror with a focal length of 1.5 m imaged through an evacuated tube. The evacuation is necessary for the VUV radiation to pass through the system. The jet is blown onto an MgF_2 window sealing the vacuum chamber. The mirror can be used to image a reference source (here, a calibrated deuterium lamp—Heraeus, Cathodeon-V03, MgF_2 window with spectral range 150–400 nm) onto the spectrograph in the same setup. The long focal length of the mirror selects only a very narrow solid angle from the plasma jet further narrowed by an aperture before the plasma jet. This ensures an almost parallel light bundle for the VUV detection and thus comparability to the deuterium lamp emission measured with the geometrically identical setup.

D. VUV absorption spectroscopy

For the VUV absorption measurements of the liquids, the same spectrograph setup was used as for the case of plasma jet VUV emission measurements with the difference that an absorption measurement cell replaced the jet. This cell is depicted in Fig. 3. In an argon filled tube, the liquid

sample is placed. The liquid sample is encapsulated inside a micro chamber (Fig. 3(b)). This micro chamber consists of a polytetrafluoroethylene (PTFE) ring of varying thickness (with a cutout for filling and taking samples), which was covered by magnesium fluoride windows on each side held together by a clamp. The chamber was always completely filled with the sample liquids taking care not to leave air bubbles trapped inside the chamber. The treatment within the micro chamber excludes all other components of the plasma jet beside (V)UV radiation. The absorption spectra of the liquids were obtained for treatment times of 1, 4, or 7 min. For accurate VUV absorption measurements, a deuterium lamp was used. This ensured a constant background radiation to gain precise absorption spectra of the different liquid films. For the absorption measurements of water vapor, the micro chamber was removed from the tube and humidified argon was guided into the tubes.

E. Hydrogen peroxide determination

The determination of hydrogen peroxide (H_2O_2) amount in ultrapure water was performed after either complete plasma jet treatment for different treatment times (20, 40, 60, 180, 360 s) of 5 ml liquid in a Petri dish or in an 80 μl micro chamber (Fig. 3(b)) with a 0.4 mm PTFE distance ring and a Plexiglas bottom. The MgF_2 window was held on top by the use of four springs and an additional PTFE ring.
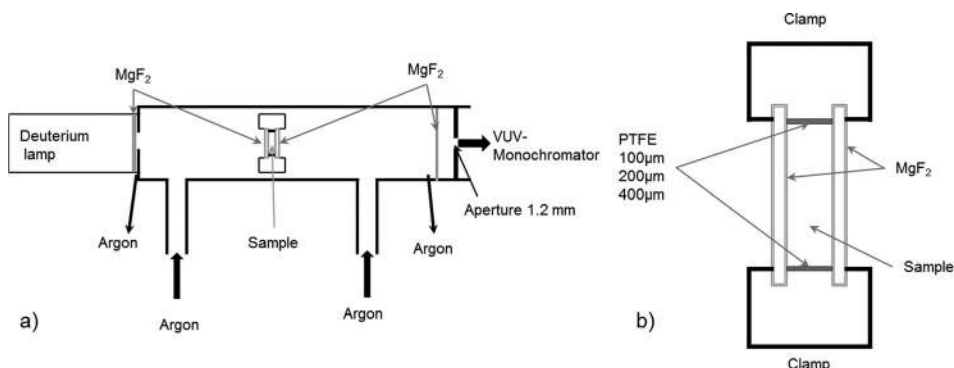

FIG. 3. Schematic drawing of (a) absorption cell for measuring transmission of liquid samples and of (b) micro chamber setup.

For the analysis of hydrogen peroxide, commercial peroxide test stripes in the range from 0.1 mg/l to 25 mg/l (Merck Millipore, Germany) have been used, assisted with a camera read-out to enhance the accuracy.[22] Before each experiment, a standard curve was measured in the investigated solutions by the use of commercial hydrogen peroxide solution (initial concentration of 9.705 M, Sigma-Aldrich, USA). The range of the performed standard curves was from 0 mg/l to 6 mg/l. Details of the measurement procedure and accuracy considerations can be found in Ref. [22].

The H_2O_2 concentration of the investigated liquids was always measured in triplets: For each sample, three test stripes were used. On each stripe, a droplet of 10 μl treated sample was pipetted, and each parameter set was repeated three times. For the comparison of these two experimental setups, the absolute number of generated hydrogen peroxide molecules was calculated from the measured concentration and the sample volume. The values presented in Section III are averaged and shown with the maximum positive and negative variance of all determined values of each parameter set.

F. Electron paramagnetic resonance spectroscopy

For qualitative and quantitative measurement of plasma generated free radicals in liquids, electron paramagnetic resonance spectroscopy (EPR), also known as electron spin resonance (ESR) or electron magnetic resonance (EMR) spectroscopy, is the method of choice.[23]

Due to the short half-life of the radicals, a chemical agent is necessary for detection. This so called spin trap was used to stabilize the radicals for sufficient time. As spin trap, here, 5,5-dimethy-1-pyrroline-N-oxide (DMPO) was used. DMPO is commonly applied to detect hydroxyl ($^\bullet$OH) and superoxide anion ($O_2^{\bullet-}$) radicals.[24] DMPO was solved in ultrapure water (100 mM) and an untreated DMPO containing sample was measured before the plasma treatment. A volume of 80 μl was treated with the kinpen for 20, 40, 60, 180, or 300 s. Each parameter set was measured for three independent samples. The used EPR spectroscope was a X-band EPR (EMXmicro, Bruker BioSpin GmbH, Germany) with an ER 4119 HS resonator where the 50 μl glass sample tube was placed inside. More information about the detailed measurement procedure and the evaluation process can be found in a previous publication.[23]

III. RESULTS AND DISCUSSION

A. (V)UV emission

The kinpen emits light from the VUV to the infrared (IR) spectral regime.[16,25] In Fig. 4, the optical emission spectrum of the kinpen is shown. In the inset, the UV to near IR (NIR), 200–850 nm, spectrum is depicted. $^\bullet$OH emission and molecular nitrogen (N_2) emission from impurities or diffusing surrounding species can be observed around 300–350 nm. In the IR, argon emission lines dominate the spectrum. Small atomic oxygen lines at 777 nm and 844 nm can be observed. The visible region from 400 to around 700 nm is mostly free of emission features.
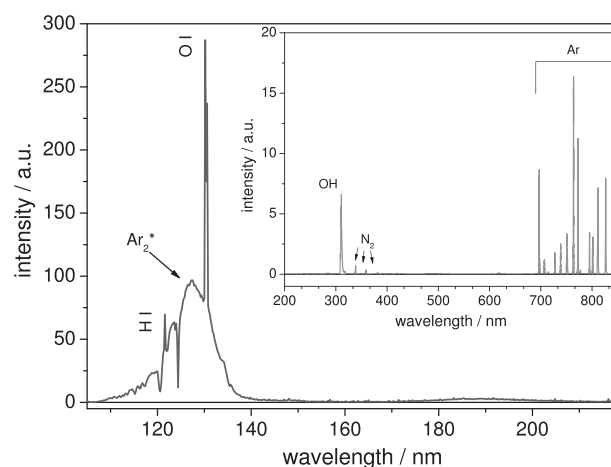

FIG. 4. VUV and UV/VIS/NIR (inset) emission of kinpen (pure Ar-discharge in ambient air).

The large spectrum shows the emission in the VUV spectral region (105–300 nm). Here, atomic oxygen and hydrogen lines were observed. In the argon excimer continuum centered around 126 nm, absorption lines of molecular oxygen and ozone can be found.[25]

Basic principles of protection against UV radiation are given in Ref. [26]. The physiological effectivity of different spectral regions between 180 and 380 nm on unprotected skin or eyes is considered there by spectral weighting factors $S(\lambda)$ to calculate the effective irradiance E_{eff} from measured values of the spectral irradiance E_λ: $E_{eff} = \sum E_\lambda \times S(\lambda) \times \Delta\lambda$. The daily effective exposure $H_{eff} = \int_t E_{eff}\, dt$ should not exceed 30 J/m^2. VUV radiation as a part of ultraviolet C (UVC, 100–280 nm) is explicitly not taken into account in this paper on the grounds that VUV is usually readily absorbed in air. With rare gas operated jet plasma sources, the situation becomes different. In the core of the plasma plume with fairly pure rare gas atmosphere where absorbing species from ambient air are absent, radiation transport of VUV photons takes place. Especially when the tip of the plasma plume is very close to the treated surface, VUV photons can interact with its boundary layer.

To our knowledge, there is no similar international guideline on UVC-VUV available; nevertheless, in Ref. [27], a suggestion is given for radiation below 180 nm. The value of $S(\lambda)$ at 180 nm in Ref. [26] has to applied constantly over the range of 100–180 nm to calculate E_{eff}, whereas the maximum daily effective exposure H_{eff} of 30 J/m^2 holds for the whole UV range of 100–380 nm.

An effective irradiance for kinpen09 was estimated by the values given in Table III. Since the applied voltage for the present study is 60 V and the working distance is 9 mm, the effective VUV irradiance is estimated to E_{eff} of 36 μW/cm^2.

For a similar plasma source which is a certified medical product, the kINPen MED$^\circledR$ in a working distance of 7–8 mm from the nozzle tip, a value E_{eff} of 35 $\pm$ 5 μW/cm^2 has been determined in the spectral range of 100–380 nm.[28] The corresponding irradiated surface element has an area of 5 mm^2. By scanning the treated area in a meander like way with the recommended speed of 60 s/cm^2, each surface element interacts for about 3 s with the plasma radiation. This leads to an

TABLE III. Total VUV irradiance from 115 to 140 nm of kinpen (6 slm argon) by variation of voltage and distance between nozzle and target is shown. The voltage applied for the present study is 60 V.

distance nozzle-target (mm)	Column total VUV irradiance (mW (cm)$^{-2}$)				
	65 V	60 V	55 V	50 V	45 V
4	17.397	17.354	16.817	16.021	14.99
6	7.524	7.401	7.341	7.006	6.694
8	3.559	3.482	3.465	3.242	3.105
10	1.879	1.959	1.877	1.616	1.55
12	1.069	1.06	0.975	0.833	0.786

effective exposure H_{eff} of 105 ± 15 μJ/cm$^2 = 1.05 \pm 0.15$ J/m^2, thus 1/30 of the maximum acceptable daily dose. Furthermore, investigations have shown that the emitted VUV radiation and the total VUV irradiance (Table III) are below harmful levels.[28] From Table I, it can be derived that the plasma jets VUV radiation carries enough energy to generate chemistry within treated biological liquids.

B. VUV absorption in liquids

In the following, absorption of VUV radiation by biological liquids is investigated and the effect of plasma jet VUV radiation on ROS generation within these liquids is studied. For the absorption spectra, as described in Section "II D," a broadband VUV deuterium lamp as light source was used in order to measure accurate absorption spectra. A spectrum of the used lamp can be found in Refs. 15 and 16. Since the kinpen is a filamentary rf excited plasma source, the absorption had to be performed with a background light source that is stable and emits over a constant area. The deuterium lamp provides these conditions, and good absorption data of the liquid films were achieved.

Fig. 5 shows the absorption spectra for different distilled water film thicknesses. The cutoff wavelength at 50% absorption is around 180 nm, for a 0.2 mm thick layer, and moves to almost 183 nm for 0.4 mm thick water layer. For wavelengths below 180 nm, almost 100% of the VUV radiation is absorbed. On the right hand side of the cutoff wavelength, the absorption is below 10%. The distilled water was
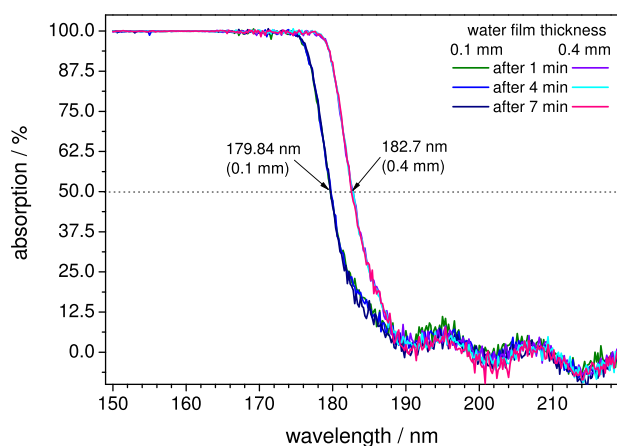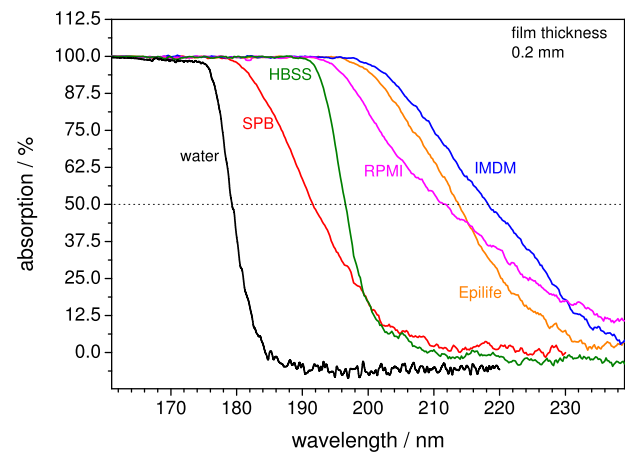

FIG. 6. VUV absorption of different liquids at 0.2 mm sheath thickness.

treated for 1 min, 4 min, and 7 min. No significant treatment time dependent difference in the absorption spectrum can be observed. The absorption spectrum for higher wavelengths is unaltered for different layer thicknesses.

Fig. 6 shows absorption spectra of the six different liquids used. Qualitatively, the liquids exhibit the same behavior: a more or less steep decrease of the absorption reaching a plateau of minimal absorption for the higher wavelengths. It can be clearly seen that the closer the liquid resembles physiological liquids, the higher is the cutoff wavelength. Distilled water has the lowest absorption cutoff wavelength and IMDM has the highest cutoff wavelength.

This becomes even more obvious, when the liquids are ranked according to the number of component groups admixed. In Fig. 7, the cutoff wavelength at 50% absorption is shown as a function of liquid complexity according to Table II. This representation is only qualitative, because surely more intricate absorption and energy dissipation processes are involved, but the trend is obvious and shows that the more component groups are present in the liquid, the higher is the absorption cutoff wavelength. This means that the more complex the liquid, the less likely it is for a VUV photon to reach a biological cell. Furthermore, with a higher absorption of higher energy photons, more photochemical processes occur along the photon pathway.

FIG. 5. Absorption of VUV radiation trough a 0.1 mm and a 0.4 mm thick water film.
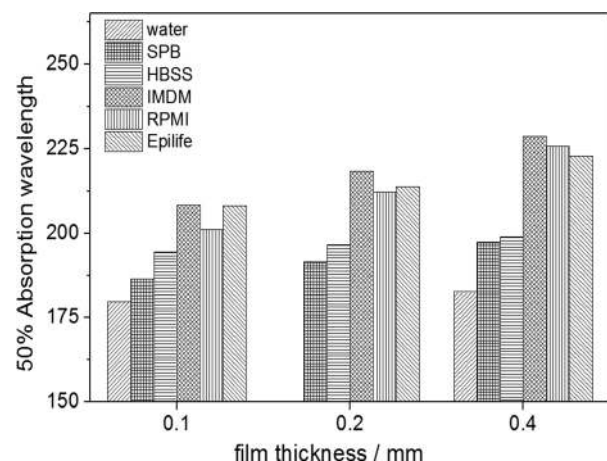

FIG. 7. Wavelength at which 50% absorption of plasma jet radiated VUV occurs of different liquids in dependency of their film thickness.
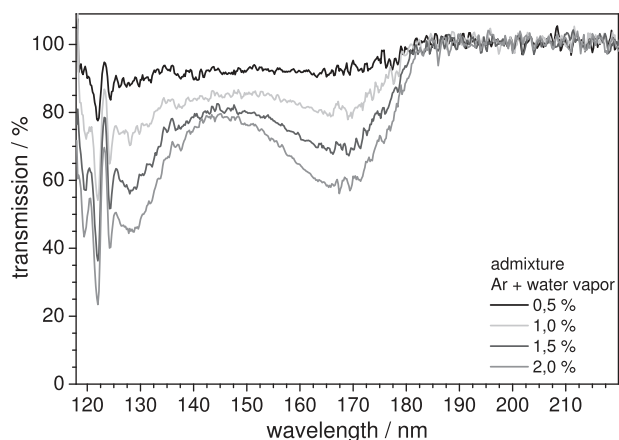
FIG. 8. VUV transmission of argon gas with different percentage of water vapor admixture. A deuterium lamp was used as a broadband VUV background source.

During treatment of liquids with the kinpen, a gradient of evaporating liquid from the bulk can be expected,[29] so that the atmosphere surrounding the plasma plume becomes humidified. This humidity has an influence on the H_2O_2 and ${}^\bullet OH$ generation.[30] To investigate the absorption of this humid atmosphere, the transmission of VUV radiation through argon gas with small admixtures of water vapor was investigated. Fig. 8 shows that with higher water vapor concentration, less VUV radiation, will be transmitted.

In Fig. 9, the VUV spectrum of the kinpen09 (black graph related to the left y-axis) is shown together with the absorption curve of a 0.4 mm thick water layer (grey graph related to the right y-axis) in the same figure. The water absorption profile cutoff wavelength is 182 nm. Due to the strong absorption of all radiation of wavelength below 180 nm, all energy of the VUV photons will therefore be incorporated in the water, resulting in a reaction cascade with further reactive species generation within the liquid.

C. Hydrogen peroxide generation

As described in Section II, the determination of hydrogen peroxide (H_2O_2) in ultrapure water was performed after either complete plasma jet treatment for different treatment

times (20, 40, 60, 180, 360 s) of 5 ml in a Petri dish or in an MgF_2 covered micro chamber with a total volume of 80 μl. With increasing treatment time, the hydrogen peroxide concentration is rising for both treatment conditions (Fig. 10).

However, the hydrogen peroxide amount formed by the complete plasma jet in dH_2O is much higher (more than two orders of magnitude) compared to that formed by plasma jets VUV radiation (Fig. 10). This behavior was expected, since additional plasma components can also generate H_2O_2 within the liquid namely, electrons or metastable species.[31] Furthermore, there is the possibility to transfer a substantial amount of gaseous hydrogen peroxide into liquids, which easily dissolves due to the high Henry's constant of H_2O_2. The important role of this effect was determined in a previous study for the same plasma source investigated here.[32] In this study, it was shown that plasma generated ${}^\bullet OH$ radicals in the gas phase are the precursors for gas phase H_2O_2 generation and that this process strongly depends on the humidity of the feed gas.

For the H_2O_2 formation due to only VUV radiation of the plasma jet, this gas phase produced hydrogen peroxide does not play a role, since the liquid volume is covered by a gas tight window during treatment. Therefore, only liquid phase species and VUV driven generation processes within the liquid are involved in the formation processes of hydrogen peroxide.

D. Formation of radicals in liquid

For the detection of plasma VUV generated oxygen radicals, namely, hydroxyl radicals (${}^\bullet OH$) and superoxide anion radicals ($O_2^{\bullet -}$), three different studies were performed. For the first treatment, the plasma jet was positioned over a Petri dish (diameter 60 mm). This Petri dish was filled with 5 ml of 100 mM DMPO in ultrapure water, and the plasma jet nozzle was placed 9 mm above the liquid surface. The VUV and UV treatments took place in the 80 μl micro chamber (Fig. 3(b)), which was covered with a magnesium fluoride (MgF_2) or a quartz glass window, respectively (see Section II D). The differences in treated liquid volumes were necessary due to handling reasons.
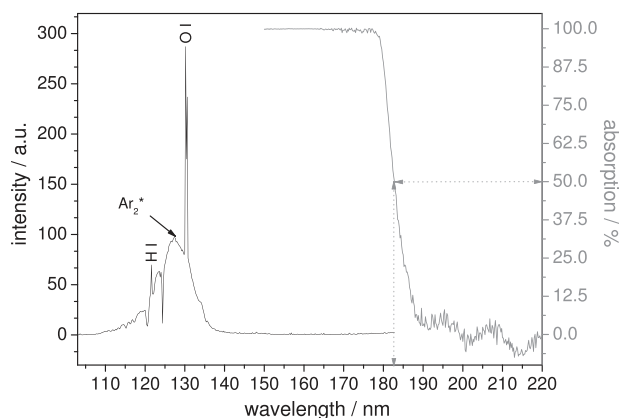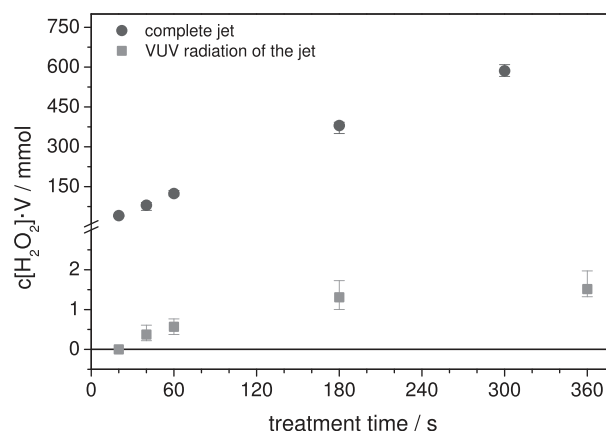

FIG. 9. Plasma jet VUV-emission (black graph) and absorption curve of VUV radiation in a 0.4 mm thick water layer (gray graph). Treatment time of the absorption experiment was 1 min.

FIG. 10. Treatment time dependency of the H_2O_2 amount multiplied with treated volume produced by either complete plasma jet treatment or plasma jet VUV radiation treatment.

In Fig. 11, the radical concentration multiplied with the treated volume is depicted in dependence of treatment time. The dark gray circles represent the determined concentration after plasma jet treatment with all of its components (complete jet); the light gray squares show the generated amount of hydroxyl and superoxide anion radicals after only VUV radiation treatment from the jet and the black triangle stands for the formed concentration after jet UV radiation treatment. The values for the VUV generated radicals are corrected by the window transmission for the wavelength 127 nm, which is 57% assuming a linear relation of photon flux and photo dissociation.

The VUV radiation of the jet plays a significant but not dominating role in the formation process of $^{\bullet}OH$ and $O_2^{\bullet -}$ radicals in ultrapure water after plasma treatment. In comparison, the UV radiation seems not to be involved in their generation during plasma treatment. The required energy for bond cleavage of the water molecule is higher than the energy provided by UV radiation of the plasma jet. Hence, UV photons do not have an essential impact on the radical generation in water. The bond dissociation energy of water (H-O-H) into O-H and H is 498.7 kJ/mol (5.17 eV)[18] and for the O–H bond into O and H the bond dissociation energy is 428 kJ/mol (4.44 eV).[18] Therefore, UV is not energetic enough for the dissociation of water and thereby is not able to generate hydroxyl radicals. The Ar_2^{*} (126 nm) instead is able to provide approximately 10 eV and thus provides more than enough energy to split the two O–H bonds in the water molecules.

In Fig. 12, the impact of the liquid ingredients during radical formation by plasma jet VUV radiation was investigated. For this, ultrapure water, Hank's buffered saline solution, and the complete cell culture medium RPMI were treated either with the complete plasma jet or with the plasma generated VUV radiation, only. The radical concentration due to VUV treatment is quite similar for all three liquids. It can therefore be deduced that additional ingredients in HBSS and in RPMI do not influence the generation of oxygen radicals by VUV radiation considerably. This leads to the conclusion that in these three solutions, the primary formation mechanism is the same—namely, dissociation of water. For the case of the
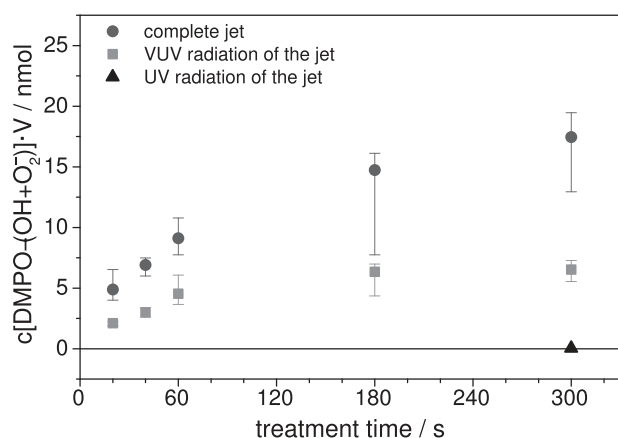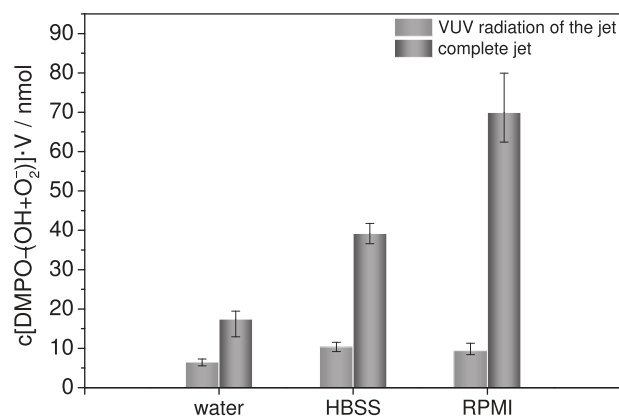

FIG. 12. Comparison of the impact of jet VUV radiation and complete plasma jet treatment (treatment time 180 s) for three different biological relevant solutions.

plasma jet treatment, the ingredients play a non-negligible role. The variation in formed oxygen radical formation due to different liquid complexity at constant plasma jet treatment conditions was already found in a previous study.[33]

Comparing the hydrogen peroxide concentrations (Fig. 10) after plasma jet VUV treatment with the oxygen radical concentrations (Fig. 11), it was found that the trends of the curves are similar. The generated H_2O_2 amount, however, is much higher than the total measured oxygen radical quantity. This is surprising, since one of the main reactions forming hydrogen peroxide is by two hydroxyl radicals (Eq. (1)) or via the reaction of superoxide anion radicals with water molecules (Eq. (2)).[34,35]

$$^{\bullet}OH + {}^{\bullet}OH \rightarrow H_2O_2, \tag{1}$$

$$2O_2^{\bullet -} + 2H_2O \rightarrow 2H_2O_2 + 2OH^- + O_2. \tag{2}$$
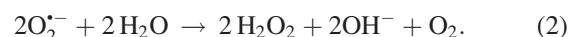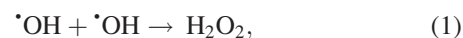
This behavior is unexpected. One possible explanation for the discrepancy is that there are other, non-radical, oxygen species involved which are responsible for hydrogen peroxide generation. A possible reaction could be from water dissociation to molecular hydrogen and oxygen

$$2H_2O \rightarrow 2H_2 + O_2 \rightarrow H_2 + H_2O_2. \tag{3}$$
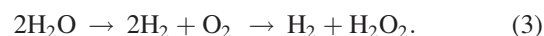
This reaction (Eq. (3)) is known and is the main reaction within the commercial hydrogen peroxide formation process called anthraquinone process, since for commercial H_2O_2 generation, a 2-alkyl-anthraquinone is used as a catalyst.[36] For the first part of Eq. (3), the two water molecules have to be cleaved.

The energies required for the reaction chain are 5.01 eV for the first part of reaction (3) and 3.76 eV for the second part. The plasma generated VUV radiation provides more than enough energy for both reactions to take place (see Table I) since plasma jet's VUV radiation of 126 nm equals 9.84 eV. However, comparing the cross sections of water dissociation into hydroxyl radical and atomic hydrogen with the cross section of water dissociation into molecular hydrogen and oxygen, the latter reaction's cross section is more than one order of magnitude lower.[37] Therefore, the probability of radical formation by photo dissociation of water is higher.

FIG. 11. Concentration multiplied with treated volume of generated oxygen radicals with taking account of MgF_2 window transmission of VUV (57%).

A second hypothesis for an explanation of the discrepancy between the hydroxyl radical production and the hydrogen peroxide production is the following. The penetration depth of VUV radiation in water is extremely low. Calculated with the Lambert-Beer-law and the absorption coefficient of Ar_2^* emission (126 nm) in water, which is in the order of $104 \, cm^{-1}$, the remaining radiation intensity is decreased to 1% after 4.6 μm depth in water; after 9.2 μm, the intensity is further decreased to 0.01%. After 30 μm, the remaining radiation drops down to 10^{-11} part of its origin. Therefore, most hydroxyl radicals will be formed directly at the liquid surface. In combination with the fact that the liquid is not stirred during VUV treatment, due to the measurement immanent separation of gas flow and liquid, and furthermore, the treatment is only spot-like, we assume that the radical formation takes place in a small volume element of 1 mm in radius (approximate radius r of the visible plasma plume) and a height h of 2 μm (due to the penetration depth of the radiation). From $[\pi \times r^2 \times h] = V = 7.8 \times 10^{-8}$ follows that the volume in which oxygen radicals can be generated is only the 7.8×10^{-8} part of the whole treated volume of 80 μl.

This affects also the hydrogen peroxide concentrations. Therefore, the measured values need to be corrected by this factor to get the formed amount in the volume element. Since hydrogen peroxide is formed by two hydroxyl radicals, the necessary $^{\bullet}$OH concentration is given by the multiplication of the H_2O_2 concentration with two. This leads to an estimated particle number of 1.56 mol locally generated in the volume element. The amount of spin trap in the small volume element is by the used concentration of 100 mM than 0.6 pmol. This is much too low to trap all generated hydroxyl radicals, since the reaction of $^{\bullet}$OH with another $^{\bullet}$OH is quite fast.[34] Hence, in the volume element, the recombination of hydroxyl radicals is dominating over the spin trap adduct formation reaction. In Ref. [38], it was found that DMPO concentrations of at least 10 mM are needed to inhibit the production of hydrogen peroxide to 43% of the case without a spin trap. The reaction rate of the spin trap DMPO with $^{\bullet}$OH is 3–5 $\times 10^9$ $M^{-1}s^{-1}$ (Ref. [39]), and the reaction rate of two hydroxyl radicals with each other is in the same order (3–6 $\times 10^9$ $M^{-1}s^{-1}$).[40,41] Theoretically the spin trap concentration needs to be increased; practically, it is not possible, since the needed amount is not solvable. In fact, oxygen free radicals were generated by plasma jet's VUV radiation and also if the measured absolute numbers are lower than in reality; still, the trend of the radicals and the trend of hydrogen peroxide are similar.

These results necessitate further investigations to clarify the formation processes of reactive species by plasma jet VUV radiation. Should the effects discussed in the second hypothesis be responsible for the discrepancies of $^{\bullet}$OH and H_2O_2 generation, an improved experimental setup needs to be developed to either enable a more homogeneous treatment of the sample volume or to be able to increase the spin trap concentration in the volume element to a concentration required to detected all locally generated oxygen radicals. An alternative is to change the spin trap to one with a higher reaction rate with hydroxyl radicals than the formation of hydrogen peroxide by two $^{\bullet}$OH molecules.

The penetration depth of the VUV radiation drops drastically with increasing liquid layer thickness, as already described. Since most wounds are covered with a thin liquid film, it is highly improbable that the VUV radiation will even reach the cells. After 25 μm, there is approximately 10^{-9}% of the radiation remaining. This was calculated by Lambert-Beer's-law and the absorption coefficient of Ar_2^* emission ($a_{126\,nm} \approx 10^{-4}$). So, if the cells are covered by at least a 25 μm thick liquid layer, it can be assumed that no VUV radiation of the plasma jet will reach the cells.

A risk estimation of plasma jet generated VUV radiation for therapeutic application the certified medical product kINPen MED® leads with the effective exposure H_{eff} of 1.05 ± 0.15 J/m^2 to merely 1/30 of the maximum acceptable daily dose.

Additionally, we found that the trend of VUV induced oxygen free radicals in complex liquids and the inhibition of human skin cells' viability[42] shows exactly the contrary behavior in dependency of the surrounding atmosphere. Thus, it can be claimed that the VUV generated ROS in the liquid are not the dominating species for inhibition of skin cell viability.

IV. SUMMARY AND CONCLUSIONS

This study showed the impact of argon plasma jet VUV radiation on the generation of reactive species in biologically relevant solutions.

In the gas phase, emission lines of argon and atomic oxygen in the infrared dominate the emission spectra of the kinpen. In the ultraviolet range, the prominent lines are related to the hydroxyl radical emission around 308 nm and to the molecular nitrogen (330–380 nm). For this study, the most interesting regime, the VUV range, was dominated by the 2nd argon excimer continuum around 126 nm. The VUV absorption spectra measured with a deuterium lamp in different liquids and also for different layer thicknesses was investigated with the result that complete VUV radiation generated by the plasma jet will be absorbed by all the liquids of all thicknesses, since the cutoff wavelength of water, which is the lowest cutoff wavelength of all liquids, is around 180 nm, depending on the layer thickness. The more complex the solutions composition is, the further the cutoff wavelength shifts to higher wavelengths. For cell culture media—the most complex of the investigated liquids—the cutoff wavelength is between 210 and 230 nm. During direct plasma jet treatment, there is always a slight evaporation of the plasma treated liquid observable by a volume and mass lost after plasma treatment (data not shown). The effect of this humidified surrounding was studied for different water vapor percentages in the air atmosphere in front of a VUV source. For the wavelength of the 2nd argon excimer, already 2% water vapor leads to a decrease of the transmission of about 50%.

The energy of the argon excimer is high enough to dissociate water forming reactive oxygen species in plasma treated liquids. The experiments show that all studied species were also formed by pure plasma jet VUV radiation treatment but in lower amounts than for the complete plasma jet

treatment. For different complex liquids, the concentration of oxygen radicals formed by VUV radiation stays constant, which leads to the conclusion that the supplementary ingredients do not contribute to the oxygen radical formation by the plasma jet's VUV radiation, so that the dissociation of water seems to be responsible for the reactive oxygen species generation.

The trend of the longer stable, non-radical species, hydrogen peroxide, and the short-lived oxygen radicals, hydroxyl and superoxide anion, is similar over treatment time, but the absolute amounts differ significantly. Due to the similar trend and the fact that H_2O_2 is known to be mainly formed by two $^{\bullet}OH$ radicals, the assumption that related processes are underlying the formation processes of both seems to be natural. Thus, the hypothesis that locally much more hydroxyl radicals were formed by plasma jet's VUV radiation than they could be trapped by the present spin trap in this volume element could explain the discrepancy in the absolute amounts of H_2O_2 and $^{\bullet}OH$. Also, additional hydrogen peroxide formation reaction could be involved, but not in the extent of the observed concentration gap. For that reason, further investigations will be necessary to clarify the obtained results from the liquid diagnostics.

It becomes almost impossible for VUV radiation to reach the cells if they are covered by a thin liquid layer of at least 25 μm, since this layer thickness left only 10^{-9}% of the VUV radiation remaining. Most wounds are already covered by a liquid (ichor or blood) film so that this will protect the living cells from VUV radiation. By the results of the here presented study, it can be concluded that the risk of the generated VUV radiation of this plasma jet for therapeutic application in plasma medicine is almost negligible.

ACKNOWLEDGMENTS

[1]J. F. Kolb, A. A. H. Mohamed, R. O. Price, R. J. Swanson, A. Bowman, R. L. Chiavarini, M. Stacey, and K. H. Schoenbach, "Cold atmospheric pressure air plasma jet for medical applications," Appl. Phys. Lett. **92**(24), 241501 (2008).

[2]K. D. Weltmann, M. Polak, K. Masur, T. von Woedtke, J. Winter, and S. Reuter, "Plasma processes and plasma sources in medicine," Contrib. Plasma Phys. **52**(7), 644 (2012).

[3]M. G. Kong, G. Kroesen, G. Morfill, T. Nosenko, T. Shimizu, J. van Dijk, and J. L. Zimmermann, "Plasma medicine: An introductory review," New J. Phys. **11**(11), 115012 (2009).

[4]H. J. Ahn, K. I. Kim, G. Kim, E. Moon, S. S. Yang, and J. S. Lee, "Atmospheric-pressure plasma jet induces apoptosis involving mitochondria via generation of free radicals," PLoS One **6**(11), e28154 (2011).

[5]T. von Woedtke, S. Reuter, K. Masur, and K.-D. Weltmann, "Plasmas for medicine," Phys. Rep. **530**(4), 291 (2013).

[6]A. Kramer, J. Lademann, C. Bender, A. Sckell, B. Hartmann, S. Münch, P. Hinz, A. Ekkernkamp, R. Matthes, I. Koban, I. Partecke, C. D. Heidecke, K. Masur, S. Reuter, K. D. Weltmann, S. Koch, and O. Assadian,

"Suitability of tissue tolerable plasmas (TTP) for the management of chronic wounds," Clin. Plasma Med. **1**(1), 11 (2013).

[7]G. Lloyd, G. Friedman, S. Jafri, G. Schultz, A. Fridman, and K. Harding, "Gas plasma: Medical uses and developments in wound care," Plasma Processes Polym. **7**(3–4), 194–211 (2010).

[8]J. Heinlin, G. Morfill, M. Landthaler, W. Stolz, G. Isbary, J. L. Zimmermann, T. Shimizu, and S. Karrer, "Plasma medicine: Possible applications in dermatology," J. Ger. Soc. Dermatol.: JDDG **8**(12), 968–976 (2010).

[9]J. Wang, X. Liu, D. Liu, X. Lu, and Y. Zhang, "Mathematical model of gas plasma applied to chronic wounds," Phys. Plasmas (1994-present) **20**(11), 113507 (2013).

[10]M. Dünnbier, A. Schmidt-Bleker, J. Winter, M. Wolfram, R. Hippler, K.-D. Weltmann, and S. Reuter, "Ambient air particle transport into the effluent of a cold atmospheric-pressure argon plasma jet investigated by molecular beam mass spectrometry," J. Phys. D: Appl. Phys. **46**(43), 435203 (2013).

[11]S. Reuter, K. Niemi, V. Schulz-von der Gathen, and H. F. Dobele, "Generation of atomic oxygen in the effluent of an atmospheric pressure plasma jet," Plasma Sources Sci. Technolo. **18**(1), 015006–1 (2009).

[12]S. Reuter, J. Winter, S. Iseni, S. Peters, A. Schmidt-Bleker, M. Dunnbier, J. Schafer, R. Foest, and K. D. Weltmann, "Detection of ozone in a MHz argon plasma bullet jet," Plasma Sources Sci. Technol. **21**(3), 034015–1 (2012).

[13]J. Waskoenig, K. Niemi, N. Knake, L. M. Graham, S. Reuter, V. Schulz-von der Gathen, and T. Gans, "Atomic oxygen formation in a radio-frequency driven micro-atmospheric pressure plasma jet," Plasma Sources Sci. Tehnol. **19**(4), 045018 (2010).

[14]E. Stoffels, R. E. J. Sladek, and I. E. Kieft, "Gas plasma effects on living cells," Phys. Scr. **T107**, 79 (2004).

[15]R. Brandenburg, H. Lange, T. von Woedtke, M. Stieber, E. Kindel, J. Ehlbeck, and K. D. Weltmann, "Antimicrobial effects of UV and VUV radiation of nonthermal plasma jets," IEEE Trans. Plasma Sci. **37**(6), 877–883 (2009).

[16]R. Foest, E. Kindel, H. Lange, A. Ohl, M. Stieber, and K. D. Weltmann, "RF capillary jet—a tool for localized surface treatment," Contrib. Plasma Phys. **47**(1–2), 119 (2007).

[17]S. Reuter, *Formation Mechanisms of Atomic Oxygen in an Atmospheric Pressure Plasma Jet Characterised by Spectroscopic Methods* (Cuvillier, 2008).

[18]M. H. Stans, "Bond dissociation energies in simple molecules," NIST Spec. Publ. **1**, 1 (1970).

[19]Y.-R. Luo and J. Kerr, *Bond Dissociation Energies*, CRC Handbook of Chemistry and Physics, Vol. 89 (CRC, 2012).

[20]K.-D. Weltmann, E. Kindel, R. Brandenburg, C. Meyer, R. Bussiahn, C. Wilke, and T. von Woedtke, "Atmospheric pressure plasma jet for medical therapy: Plasma parameters and risk estimation RID G-6504-2011," Contrib. Plasma Phys. **49**(9), 631 (2009).

[21]S. Iseni, A. Schmidt-Bleker, J. Winter, K. D. Weltmann, and S. Reuter, "Atmospheric pressure streamer follows the turbulent argon air boundary in a MHz argon plasma jet investigated by OH-tracer PLIF spectroscopy," J. Phys. D: Appl. Phys. **47**(15), 152001 (2014).

[22]J. Winter, K. Wende, K. Masur, S. Iseni, M. Dunnbier, M. U. Hammer, H. Tresp, K. D. Weltmann, and S. Reuter, "Feed gas humidity: A vital parameter affecting a cold atmospheric-pressure plasma jet and plasma-treated human skin cells," J. Phys. D: Appl. Phys. **46**(29), 295401 (2013).

[23]H. Tresp, M. U. Hammer, J. Winter, K. D. Weltmann, and S. Reuter, "Quantitative detection of plasma-generated radicals in liquids by electron paramagnetic resonance spectroscopy," J. Phys. D: Appl. Phys. **46**(43), 435401 (2013).

[24]B. Halliwell and J. M. C. Gutteridge, *Free Radicals in Biology and Medicine* (Oxford University Press, Oxford, 2007).

[25]S. Reuter, J. Winter, A. Schmidt-Bleker, D. Schroeder, H. Lange, N. Knake, V. Schulz-von der Gathen, and K. D. Weltmann, "Atomic oxygen in a cold argon plasma jet: TALIF spectroscopy in ambient air with modelling and measurements of ambient species diffusion," Plasma Sources Sci. Technol. **21**(2), 024005 (2012).

[26]I. C. o. and N.-I. R. Protection, "Guidelines on limits of exposure to ultraviolet radiation of wavelengths between 180 nm and 400 nm (incoherent optical radiation)," Health Phys. **87**(2), 171–186 (2004).

[27]B. der Feinmechanik, "Elektrotechnik: Expositionsgrenzwerte für künstliche optische Strahlung," in *Berufsgenossenschaftliche Informationen für Sicherheit und Gesundheit bei der Arbeit* (HVBG in cooperation with Carl Heymanns Verlag, 2004).

[28]R. Bussiahn, N. Lembke, R. Gesche, T. von Woedtke, and K.-D. Weltmann, "Plasma sources for biomedical applications," HygMed **38**(5), 212–216 (2013).

[29]S. A. Norberg, W. Tian, E. Johnsen, and M. J. Kushner, "Atmospheric pressure plasma jets interacting with liquid covered tissue: touching and not-touching the liquid," J. Phys. D: Appl. Phys. **47**(47), 475203 (2014).

[30]S. Reuter, J. Winter, S. Iseni, A. Schmidt-Bleker, M. Dunnbier, K. Masur, K. Wende, and K.-D. Weltmann, "The influence of feed gas humidity versus ambient humidity on atmospheric pressure plasma jet-effluent chemistry and skin cell viability," IEEE Trans. Plasma Sci. **43**, 3185 (2014).

[31]S. Bekeschus, S. Iseni, S. Reuter, K. Masur, and K.-D. Weltmann, "Nitrogen shielding of an argon plasma jet and its effects on human immune cells," IEEE Trans. Plasma Sci. **43**(3), 776–781 (2015).

[32]J. Winter, H. Tresp, M. U. Hammer, S. Iseni, S. Kupsch, A. Schmidt-Bleker, K. Wende, M. Dünnbier, K. Masur, K.-D. Weltmann, and S. Reuter, "Tracking plasma generated H_2O_2 from gas into liquid phase and revealing its dominant impact on human skin cells," J. Phys. D: Appl. Phys. **47**(28), 285401 (2014).

[33]H. Tresp, M. U. Hammer, K.-D. Weltmann, and S. Reuter, "Effects of atmosphere composition and liquid type on plasma-generated reactive species in biologically relevant solutions," Plasma Med. **3**(1–2), 45 (2013).

[34]G. Czapski, "Reaction of ˙OH," Methods Enzymol. **105**, 209 (1984).

[35]B. Halliwell, *eLS* (John Wiley & Sons, Ltd., 2001).

[36]J. M. Campos-Martin, G. Blanco-Brieva, and J. L. Fierro, "Hydrogen peroxide synthesis: an outlook beyond the anthraquinone process," Angew. Chem. **45**(42), 6962 (2006).

[37]W. Huebner and C. Carpenter, US Government Printing Office, 1979.

[38]B. E. Britigan, T. L. Roeder, and G. R. Buettner, "Spin traps inhibit formation of hydrogen peroxide via the dismutation of superoxide: implications for spin trapping the hydroxyl free radical," Biochim. Biophys. Acta **1075**(3), 213 (1991).

[39]E. Finkelstein, G. M. Rosen, and E. J. Rauckman, "Spin trapping— Kinetics of the reaction of superoxide and hydroxyl radicals with nitrones," J. Am. Chem. Soc. **102**(15), 4994 (1980).

[40]G. V. Buxton, C. L. Greenstock, W. P. Helman, and A. B. Ross, "Critical-review of rate constants for reactions of hydrated electrons, hydrogen-atoms and hydroxyl radicals (˙OH/O–) in aqueous-solution," J. Phys. Chem. Ref. Data **17**(2), 513–886 (1988).

[41]A. J. Elliot, "A pulse-radiolysis study of the temperature-dependence of reactions involving H, Oh and E-Aq in aqueous-solutions," Radiat. Phys. Chem. **34**(5), 753 (1989).

[42]S. Reuter, H. Tresp, K. Wende, M. U. Hammer, J. Winter, K. Masur, A. Schmidt-Bleker, and K. D. Weltmann, "From RONS to ROS: Tailoring plasma jet treatment of skin cells," IEEE Trans. Plasma Sci. **40**(11), 2986 (2012).